The shock response of apatite and its effect on volatiles in eucrites

Conference or Workshop Item

THE SHOCK RESPONSE OF APATITE AND ITS EFFECT ON VOLATILES IN EUCRITES. T. J. Barrett[1], A. Černok[1], G. Degli-Alessandrini[1], X. Zhao[1], M. Anand[1,2], I. A. Franchi[1] and J. Darling[3]. [1]School of Physical Sciences, The Open University, Walton Hall, Milton Keynes, MK7 6AA, UK (E-mail: thomas.barrett@open.ac.uk), [2]Department of Earth Sciences, The Natural History Museum, London, SW7 5BD, UK, [3]School of the Environment, Geography & Geosciences, University of Portsmouth, Portsmouth, PO1 3QL, UK.

Introduction: The abundance and isotopic composition of volatile elements in meteorites are critical for understanding planetary evolution given their importance in a variety of geochemical processes (e.g. [1]). As such, there has been significant interest in the mineral apatite, which is known to contain appreciable amounts of volatile elements. Because shock-induced deformation is pervasive in meteorite samples, it is important to determine if the process has affected their volatile abundance and isotopic composition.

Electron Backscatter Diffraction (EBSD) analyses provide crystallographic information at the µm and sub-µm length scales. Recently, greater complexity in microscale deformation features with increasing shock pressure has been observed in phosphate minerals [2–4] and its effect on the abundance and isotopic composition of H has been explored [5].

In this study we investigate the potential linkage between µm-scale shock structures of apatite grains from six eucrites across a broad range of shock stages (S1–S5) using EBSD combined with NanoSIMS volatile abundance and isotopic composition of hydrogen and chlorine.

Samples: The samples selected, in order of shock grade, are as follows: Dar al Gani (DaG) 945 (S1), Millbillillie (S2), Stannern (S2), Puerto Lápice (S3), Cachari (S4) and Padvarninkai (S5).

Methods: The lattice orientation and internal microstructure of apatite grains were investigated using EBSD on a Zeiss Supra 55VP FEG-SEM equipped with an Oxford Instruments EBSD detector located at The Open University (OU). The step size used ranged from 300 nm to 750 nm with binning ranging from 2×2 pixels to 4×4 pixels. Generated electron backscatter patterns were matched to a hexagonal unit cell [6]. Results were processed using Oxford Instruments HKL Channel 5 software. The H and Cl volatile abundance and isotopic composition in apatite were measured using the Cameca NanoSIMS 50L at the OU in scanning ion imaging mode and spot mode for Cl and H, respectively. Both sets of analyses are based on well-established protocols [e.g. 7–9]. Measured D/H ratios are spallation corrected.

Results and Discussion: A total of 23 EBSD maps were collected for 27 individual apatite grains across the six eucrites (Fig. 1). A total of 19 Cl measurements and 17 correlated H measurements were made on 12 apatite grains from the higher shock samples (S3–S5) and combined with literature data for lower shocked samples (Fig. 2) [7, 10].

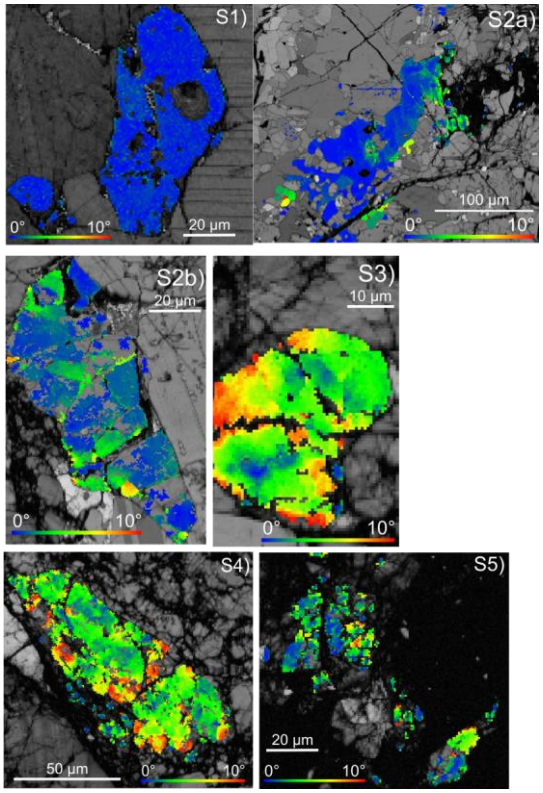

Figure 1: EBSD Band Contrast (BC) images overlain with Grain Reference Orientation Deviation (GROD) maps of apatite with progressive shock deformation. S2 (a): Stannern, S2(b): Millbillillie.

At stage S1, apatite in EBSD occur as single crystals with high BC values, a measure of diffraction pattern quality, with no obvious signs of internal deformation in GROD as anything <2° can be considered 'strain free' (Fig. 1). Pole Figures (PF) show tight clustering of orientation data (~3°). As such, these grains are considered strain free and have comparable levels of strain to unshocked terrestrial igneous apatite. H data for DaG 945 [7] are invariant both within the sample and when compared to samples of higher shock grades (Fig. 2). Chlorine, on the other hand, displays a significantly ^{37}Cl-rich signature [10]. Given the undeformed nature of apatite grains, however, it is unlikely the elevated signature was caused by shock deformation and more likely caused by another process such as magmatic degassing [10].

For S2, samples show incipient brecciation, with fractures forming a network of sub-linear features cross-cutting the apatite, with no obvious preferred orientation. The broken blocks of apatite typically have

low to no relative misorientation between each other in EBSD (typically <5˚). Stannern, however, appears to display some evidence of early stage subgrain formation (although the majority are low angle boundaries, i.e., <10˚, and appear to follow cracks). Regarding volatiles, neither mineral fracturing, nor the presence of local misorientations within the whole grain appear to correlate with the abundance and isotopic composition of Cl and H in these samples (Fig. 2). Given the low post-shock temperature (20–50 °C [11]) and slow diffusion of volatiles in apatite at < 200 °C [12], it is unlikely the slightly elevated temperatures permitted diffusion of volatiles in S2 apatite, even if fractures could have provided the pathways [9].

S3–S4 apatite show lower BC values and appear more granular than S1 and S2, as indicated by degradation of the Kikuchi patterns. Both Puerto Lápice and Cachari show an increase in the density of subgrain boundaries and PFs for these samples can show a spread up to ~30° in misorientations indicative of crystal-plastic deformation, with Cachari showing greater misorientation than Puerto Lápice. Given the lack of melt veins in this particular section, post-shock heating in Puerto Lápice is likely low (~100–150 °C [11]) and too low to allow for shock-induced diffusion of volatiles, especially as there is no increase in volatile variability (Fig. 2). Cachari, however, likely experienced higher temperatures than those modelled in [11] but lower than temperatures that show rapid H diffusion (500–700 °C [13]). Given the similarity in both H and Cl abundance and isotopic composition between the two meteorites (Fig. 2), as well as with those of lower shock (S1–S2), it is likely the volatile composition of Cachari is primary.

At the highest levels of shock deformation in the studied samples (S5), apatite is commonly in direct contact with, or near, a diaplectic plagioclase glass and reveals extensive subgrain formation and potentially recrystallisation (as outlined by the fragmental domains in BC maps not observed in BSE). S5 apatite grains display up to ~60° of continuous spread in orientation in PF, however, there is significant intra-sample variation, possibly suggesting some apatite was more effectively shielded from shock than others [11]. Padvarninkai displays a significantly more variable H_2O content and isotopic composition, with the lightest isotopic composition ($\delta D = -157 \pm 155$ ‰) located in a particularly complex region in BC. Whilst the $\delta^{37}Cl$ value for this grain is low, it is not anomalously low nor the lowest in the sample; the Cl content is also homogenous. There is also no obvious relationship between deformation in GROD, δD, and H_2O content. Diffusion modelling for this sample suggests that even at the higher post-shock temperature experienced by Padvarninkai, H would not have diffused out of the grain (~1.5 nm; based on 700 °C for 70 ms [13, 14]). Given this and the overall similarity to literature values from lower shock samples (Fig. 2), it would suggest that diffusion was either 1) not extensive, 2) the post-shock elevated temperature did last long enough for volatile diffusion or 3) the post-shock heating experienced by apatite was lower than anticipated based on the shock classification.

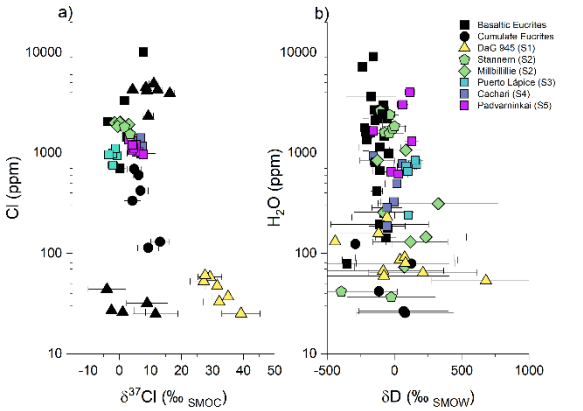

Figure 2: a) $\delta^{37}Cl$ values vs. Cl (ppm) b) δD values vs. H_2O (ppm). Literature values from [9, 11, 12, 15, 16].

Conclusion: Overall, EBSD maps display progressively larger variations in internal misorientation with increasing shock, in a similar manner to those observed by Černok et al. [2]. This increasing misorientation, however, does not correlate with either elemental abundance or isotopic composition observed at either an inter- or intra-grain scale. Results from this study are consistent with observations in water-rich highland lunar apatite [5], but differ from that of martian apatite [17]. As such, H and Cl loss and isotopic perturbations associated with shock seem to be a feature currently unique to celestial bodies with atmospheres and/or more extensive past fluid-rock interaction; i.e., Mars. Apatite, therefore, may well be a robust recorder of Cl and H on airless bodies, where there is no interaction with external sources, despite intensive shock.

References: [1] McCubbin F. & Barnes J. J (2019) *EPSL*, 526:115771. [2] Černok A. et al. (2019) *MAPS*, 54:1262-1282. [3] Cox M. A. et al. (2020) *MAPS* 55:1715-1733. [4] McGregor M. et al. (2021) *Contrib Min. Pet.* 176. [5] Černok A. et al. (2020) *EPSL* 544:116364. [6] Wilson R. M. et al (1999) *Am. Min.* 84:1406-1414. [7] Barrett T. J. et al. (2016) *MAPS* 51:1110-1124. [8] Stephant A. et al. (2019) *EPSL*, 523:115715. [9] Barrett T. J. et al. (2021) *GCA*, 302:120-140. [10] Barrett T. J. et al (2019) *GCA*, 266:582-597. [11] Fritz J. et al (2017) *MAPS* 52:1216-1232. [12] Brenan J. M. (1993) *Chem. Geol.* 110:195-210. [13] Higashi Y. (2017) *Geochem.* 51:115-122. [14] Ozawa S. et al. (2014) *Sci. Rep.* 4:5033. [15] Sarafian A. R. et al. (2014) *Science* 346:623-626. [16] Sarafian A. R. et al. (2017) *EPSL* 459:311-319. [17] Darling J. R. et al. (2021) *GCA* 293:422-437.